ergy

SOLAR

DOE/JPL/1060-76
(DE85000352)

EXPERIMENTAL AND THEORETICAL STUDY OF A SOLAR THERMOCHEMICAL RECEIVER MODULE

By
Y. S. Won
G. E. Voecks
J. H. McCrary

July 15, 1984

Work Performed Under Contract No. AM04-80AL13137

Jet Propulsion Laboratory
Pasadena, California

Technical Information Center
Office of Scientific and Technical Information
United States Department of Energy

DISCLAIMER

Available from the National Technical Information Service, U. S. Department of Commerce, Springfield, Virginia 22161.

Price: Printed Copy A03
Microfiche A01

Codes are used for pricing all publications. The code is determined by the number of pages in the publication. Information pertaining to the pricing codes can be found in the current issues of the following publications, which are generally available in most libraries: *Energy Research Abstracts (ERA); Government Reports Announcements* and Index *(GRA* and I); *Scientific and Technical Abstract Reports (STAR);* and publication NTIS-PR-360 available from NTIS at the above address.

Printed in the United States of America
USDOE Office of Scientific and Technical Information
Oak Ridge, Tennessee

5105-139
Solar Thermal Power Systems Project
Parabolic Dish Systems Development

DOE/JPL/1060-76
(JPL-PUB-84-53)
(DE85000352)
Distribution Category UC-62b

Experimental and Theoretical Study of a Solar Thermochemical Receiver Module

Y.S. Won
G.E. Voecks
J.H. McCrary, New Mexico State University

July 15, 1984

Prepared for
U.S. Department of Energy
Through an Agreement with
National Aeronautics and Space Administration
by
Jet Propulsion Laboratory
California Institute of Technology
Pasadena, California

JPL Publication 84-53

ABSTRACT

A few years ago, a prototype test module of a solar thermochemical receiver using an SO_2/SO_3 reaction system was designed, built, and tested to establish a technical data base for future subsystem design efforts. Emphasis was placed on experimental verification of the computer simulation to establish a reliable design tool to predict the thermochemical performance of the receiver with a reasonable degree of confidence. The computational results were compared with experimental results obtained from the module tested at New Mexico State University. Reasonable agreement was found over a range of test conditions. It was concluded that the present design offers satisfactory conversion performance and operational flexibility for the construction of a complete reactor/receiver unit for use in a 10- to 15-kW dish collector system.

ACKNOWLEDGMENT

The work described herein was conducted by the Jet Propulsion Laboratory, California Institute of Technology, for the U.S. Department of Energy through an agreement with the National Aeronautics and Space Administration (NASA Task RE-152, Amendment 327; DOE/ALO/NASA Interagency Agreement No. DE-AM04-80AL13137).

NOMENCLATURE

A	cross-sectional area of the tube, m^2
a_v	catalyst surface area per unit bed volume, m^2/m^3
C_l	bulk concentration of reactant in the fluid stream, kg-mole/m^3
$C_{l,s}$	reactant concentration at the catalyst surface, kg-mole/m^3
$C_{l,e}$	equilibrium concentration of reactant, kg-mole/m^3
C_p	specific heat of fluid, J/kg^oK
D_t	reactor tube diameter, m
D_p	catalytic particle diameter, m
G	mass flow rate per unit area, kg/s m^2
h_f	convective heat transfer coefficient between catalyst and fluid, W/m^{2o}K
$H_{R,v}$	heat of reaction per unit bed volume, J/m^3s
k_f	thermal conductivity of gas mixture, W/m^oK
k_g	mass transfer coefficient between fluid and catalyst, kg-mole/m/s
k_s	reaction constant, kg-mole/m/s
$\dot{m}$	mass flow rate, kg/s
μ	viscosity, kg/m s
Nu	Nusselt number
ρ_f	fluid density, kg/m^3
T_f, T_s, T_w	temperatures of fluid, catalyst surface, and tube wall, respectively, ^oC
T_w'	insulated wall temperature, ^oC
Q_R	solar radiant heat flux, W/m^2
U	overall heat transfer coefficient between the heat-receiving surface and fluid, W/m^oK

CONTENTS

Figures

Table

SECTION 1

INTRODUCTION

Use of reversible chemical reactions as a means of transporting and storing solar thermal energy is a promising research and development area. Various thermochemical systems have been suggested. These systems, each with its own merits and shortcomings, were at various stages of development at the time this work was performed.

Although the identification of the most promising reaction system for a specific application is important, it is equally important that the techno-economic feasibility of the proposed system be assessed at an early stage of development. In assessing a system, however, the parameters normally used are primarily projections because little actual test information is available at the present time. Overly optimistic assumptions or inadequate treatment of potential systems problems may lead to erroneous conclusions and result in a waste of time and effort. Generation of more realistic performance data by fabricating and testing the actual hardware (scaled down in size) is essential for effective planning of the overall development effort.

The intent of this study was (1) to demonstrate the concept's technical feasibility by developing reliable design tools and identifying any outstanding problems and (2) to generate reliable performance data required for an economic feasibility study. The thermochemical system chosen for the present study is one based on the catalyzed sulfur trioxide dissociation reaction

$$SO_3 \rightleftharpoons SO_2 + O_2 \qquad (1)$$

initially proposed by Chubb (Refs. 1 and 2).

Technical feasibility primarily involves the determination of the catalytic activity of a particular reactor design and catalyst, and the reactor/catalyst material compatibility with reactants. As a first step toward this effort, a small test module was designed and fabricated by the Jet Propulsion Laboratory (JPL), and tested at New Mexico State University. This module would conceivably be one element in a reactor/receiver that features a stack of these double-tube coils, of which the innermost layers form a heat-receiving cavity.

SECTION II

TEST MODULE DESIGN

The feasibility demonstration of the prototype metal reactor was to be conducted in a solar environment with the Omnium-G collector installed at the JPL Parabolic Dish Test Site in the Mojave Desert, California. Therefore, the reactor capacity was based on the thermal power input obtainable by a collector of the size comparable to Omnium-G (OG-7500), i.e., 12.5 kW_t with an 8-in. aperture at an insolation of 1.0 kW/m^2. Assuming a receiver efficiency of 80%, the thermal power input was estimated to be 10 kW_t. From a materials viewpoint, the maximum cavity wall temperature was limited to 900°C. Approximate sizing followed by detailed analysis, using a computer program, produced a design encompassing a cavity, 12 in. in diameter and 20 in. long, formed by 20 circular reactor rings of 1-in. stainless steel tubing. Each reactor ring, packed with catalyst, was connected to a spiral double-tube heat exchanger, having a total of 5 1/2 turns.

The reactor was made of one piece of 1-in. diameter tubing, 38 in. long, and formed into a 12-in. diameter circle. At 5-in. intervals on the tube surface, orthogonal to the plane, 1/16-in. Swagelok fittings were welded for instrumenting with thermocouples. Swagelok fittings (1/16 in.) were also welded to the two right-angle Swagelok elbows on the out-of-plane surface for thermocouple instrumentation. These elbows were also fitted with a stainless steel wire mesh screen to retain the catalyst. The reactor was filled with platinum catalyst deposited on spherical aluminum oxide substrate.

Thermocouples (K type, stainless steel sheath, 1/16-in. diameter, 18 in. long) were inserted approximately 1/4 in. into the catalyst bed and tightened into position for gas phase temperature monitoring at the inlet, outlet, and incrementally along the reaction path. In addition, thermocouples were attached to the outside wall of the reactor on the inside and outside of the circle to monitor the heated wall temperature and the temperature differential across the tube during operation.

The heat exchanger spiral was fabricated from tubing 5/8 in. and 1 in. in diameter and 38 ft long. A stainless steel wire (1/8-in. diameter) was wrapped around the smaller tubing and inserted together into the larger tubing prior to winding them 5 1/2 turns. The tubing ends on the inside of the spiral were positioned to match the reactor's 1-in. Swagelok fittings. The outside tubing was welded shut around the inside tube, and 1-in. Swagelok fittings were welded onto both ends to permit easy installation of the reactor. The resulting configuration allowed the reactor to be easily connected to the heat exchanger without disturbing either the catalyst or the position of the heat exchanger.

During testing, the reactant flowed through the annular passage of the spiral where it was preheated prior to entering one end of the reactor ring. The product gases and unreacted reactant exited the other end of the reactor after one pass and flowed through the inner tube of the double-tube heat exchanger to the exit.

SECTION III

DESIGN ANALYSIS AND MODEL DEVELOPMENT

A performance simulation computer program has been developed for the conceptual reactor designs currently being considered. The program, called Chemical Receiver Analysis Method (CRAM), is designed for the analysis of a single-layer reactor section and heat exchanger section, with the incoming reactants in the annulus being heated by the exiting reaction products. The reactor layer is either double-tube with the inside wall of the outer tube coated with catalyst, or single-tube packed with catalyst.

For the purpose of confining the complexity of the problem to the degree necessary for reasonable performance prediction, a one-dimensional, steady-state analysis was made with a number of simplifying assumptions as listed below:

(1) No cosine effect of impinging radiant energy along the semicircumference of the tube.

(2) Negligible axial conduction compared with radial conduction across the tube.

(3) No end effect of the flow.

(4) Negligible radiative heat transfer in the case of packed bed reactor.

(5) Reaction rate is first-order in relation to the concentration difference between surface concentration and equilibrium.

In terms of an example of a packed bed reactor, assuming the conditions listed above, the one-dimensional governing equations are as follows:[1]

(1) Energy Balance

$$G \frac{d}{dx} (C_p T_f) + h_f a_v (T_f - T_s) - 2 \frac{U}{D_t} (T_w - T_f) = 0 \qquad (2)$$

$$h_f a_v (T_f - T_s) - \Delta H_{R,v} = 0 \qquad (3)$$

$$2 \frac{U}{D_t} (T_w - T_f) - \frac{2}{D_t} Q_R = 0 \qquad (4)$$

---

[1]Refer to Nomenclature for definition of terms used in the equations.

$$2\,\frac{U}{D_t}\,(T_w' - T_f) = 0 \tag{5}$$

(2) Species Balance

$$\frac{G}{\rho_f}\,\frac{dC_1}{dx} + k_g a_v (C_1 - C_{1,s}) = 0 \tag{6}$$

$$k_g(C_1 - C_{1,s}) = k_s(C_{1,s} - C_{1,e}) = r \tag{7}$$

This set of simultaneous equations was solved numerically using a library subroutine. The program versatility is provided by analyzing the heat exchanger section and reactor section separately and by effecting most of the calculations in subroutines rather than in the main program. The flow chart of the program is shown in Figure 3-1. The program run begins by reading the input data and assigning initial estimates to the temperature and concentration profiles. The program then evaluates the temperature profile in the heat exchanger section by solving the heat balance equations with coefficients based on the assumed conditions. The temperature profile for the reactor section is then determined based on the inlet stream temperature and assumed concentration profile. Mass diffusion and reaction kinetics provide the estimation of coefficients in species conservation equations. Newly calculated values continuously improve the previous values until they finally converge. Once the converged profiles of the reactor are obtained, the interface conditions between the heat exchanger and the reactor are checked. To control the stability of the convergence, a relaxation method was employed using an appropriate relaxation factor.

Thermophysical properties of the gas mixture are estimated using the properties of individual pure components and the mixing rule. The diffusion coefficient of the reactant gas in the mixture is estimated using the Maxwell concept and the Chapman-Enskog equation for the binary diffusion coefficient. The convective heat transfer coefficient in the packed bed reactor was estimated using the correlation presented by Leva (Ref. 3).

$$Nu = \frac{h_f D_t}{k_f} = 0.813\ (Re)^{0.9}\ \exp(-6D_p/D_t)\ \text{for}\ \frac{D_p}{D_t} < 0.35 \tag{8}$$

where $Re = (D_p G)/\mu$.

Based on work by Reynolds (Ref. 4), the asymetrical heating of the reactor tube wall was approximately accounted for by estimating an effective convective heat transfer coefficient between the reactor wall and the bulk of the fluid. For the reaction rate equation for SO_3 dissociation, the Westinghouse data (Ref. 5) deduced by Rocket Research in terms of catalytic surface area (Ref. 6) was used.

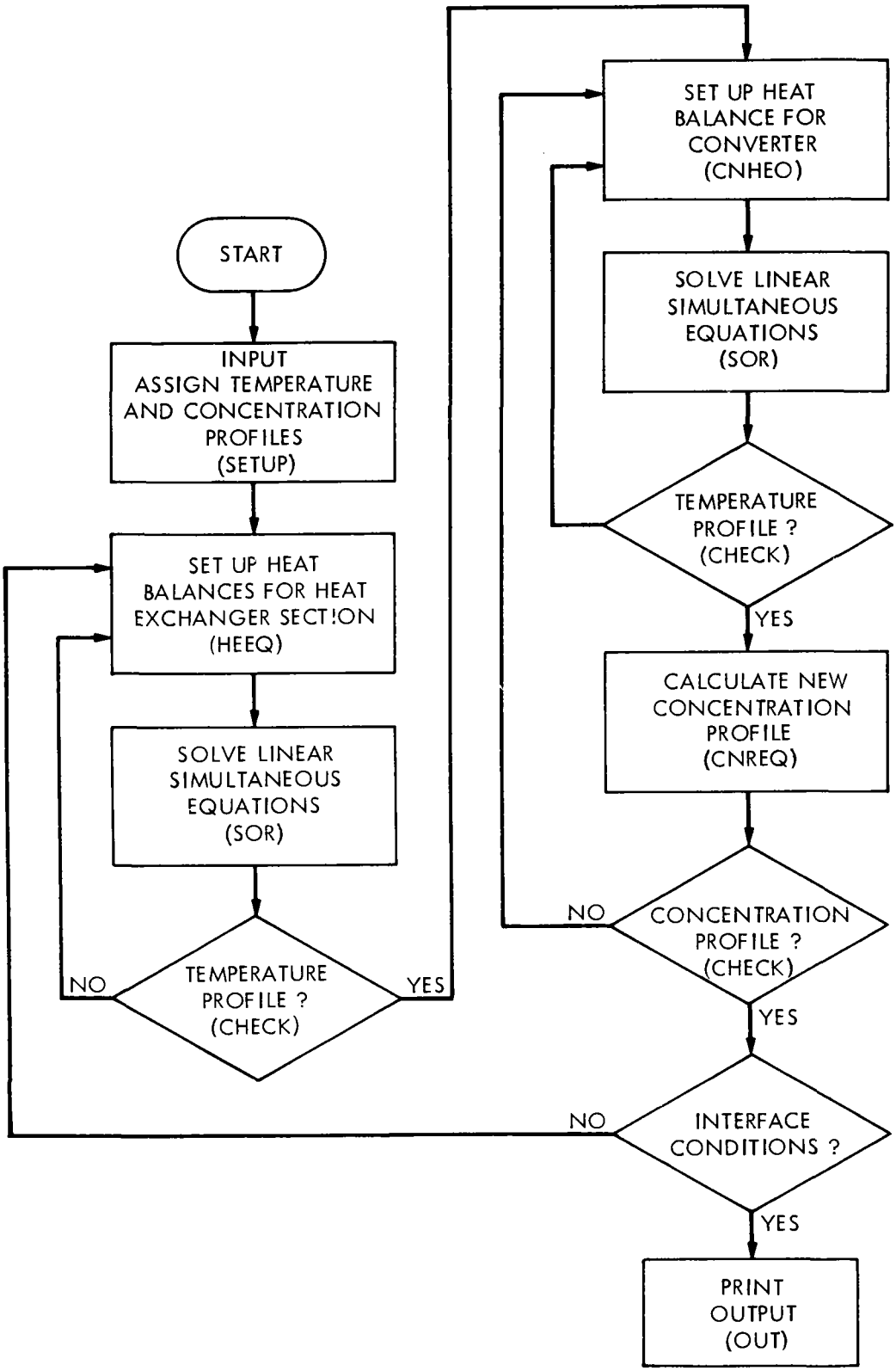

Figure 3-1. Flowchart of CRAM

SECTION IV

EXPERIMENTAL

The test module designed and fabricated at JPL was tested at a solar chemical receiver test facility belonging to the Physical Science Laboratory of New Mexico State University. A detailed description of the facility is found elsewhere (Ref. 7).

The facility features three major units: SO_3 storage and vapor supply unit, testing unit, and effluent gas disposal unit. The SO_3 storage and vapor supply unit consists of a temperature-controlled hot box containing a 55-gal liquid SO_3 drum, metering pump, and evaporator of the heated pressure-vessel type with an electronic temperature controller. The testing unit consists of the reactor, insulation, heated cavity, heating elements, and gas analyzer. The gas disposal unit is of an agricultural scrubber type described by Miyamoto, et al (Ref. 8). A schematic of the experimental test setup is shown in Figure 4-1.

Prior to the dissociation test, the reactor module as well as connecting plumbing was leak tested by pressurizing with nitrogen gas up to 60 psia; the heat exchanger thermal performance was tested at a predetermined test condition. For the dissociation reaction, the test procedure followed three steps: start-up, operation, and normal shutdown.

The liquid SO_3, maintained at a constant temperature, was pumped into the electrically heated evaporator at a regulated flow rate. A magnetically coupled gear pump constructed from stainless steel and Teflon was used. The evaporator is a custom built, heated pressure-vessel type made of stainless steel with a 2-liter capacity. The lid is removable and is equipped with a Teflon seal. An electronic temperature controller maintained the liquid phase temperature in the range of 50 to 100°C. The vapor from evaporation is carried through a 1/2-in. stainless steel tube, which is metered into the converter/heat exchanger.

The pressures were measured by absolute pressure transducers, of which analog voltage signals were recorded in the data logger. Temperatures were measured by the sheathed chromel-alumel thermocouples positioned either externally at the reactor wall or internally at the center of the flow passages. The thermocouple sensors are connected directly to the data logger, which records the gas temperatures in degrees centigrade (°C). The thermocouple map is shown in Figure 4-2.

The effluent gas leaving the reactor is carried directly to the scrubber, with a fraction of the effluent gas flowing through the gas analyzer. In addition to the effluent gas analysis, the local concentrations of SO_2 gas along the reactor bed were also measured in order to investigate the reactivity of the catalyst used. Gas samples were tapped from the equally spaced thermocouple ports along the reactor length. The SO_2 analyzer is a Dupont Model 400 ultraviolet-absorption, continuous-flow gas analyzer. This instrument measures the volume fraction of SO_2 present in the sample gas.

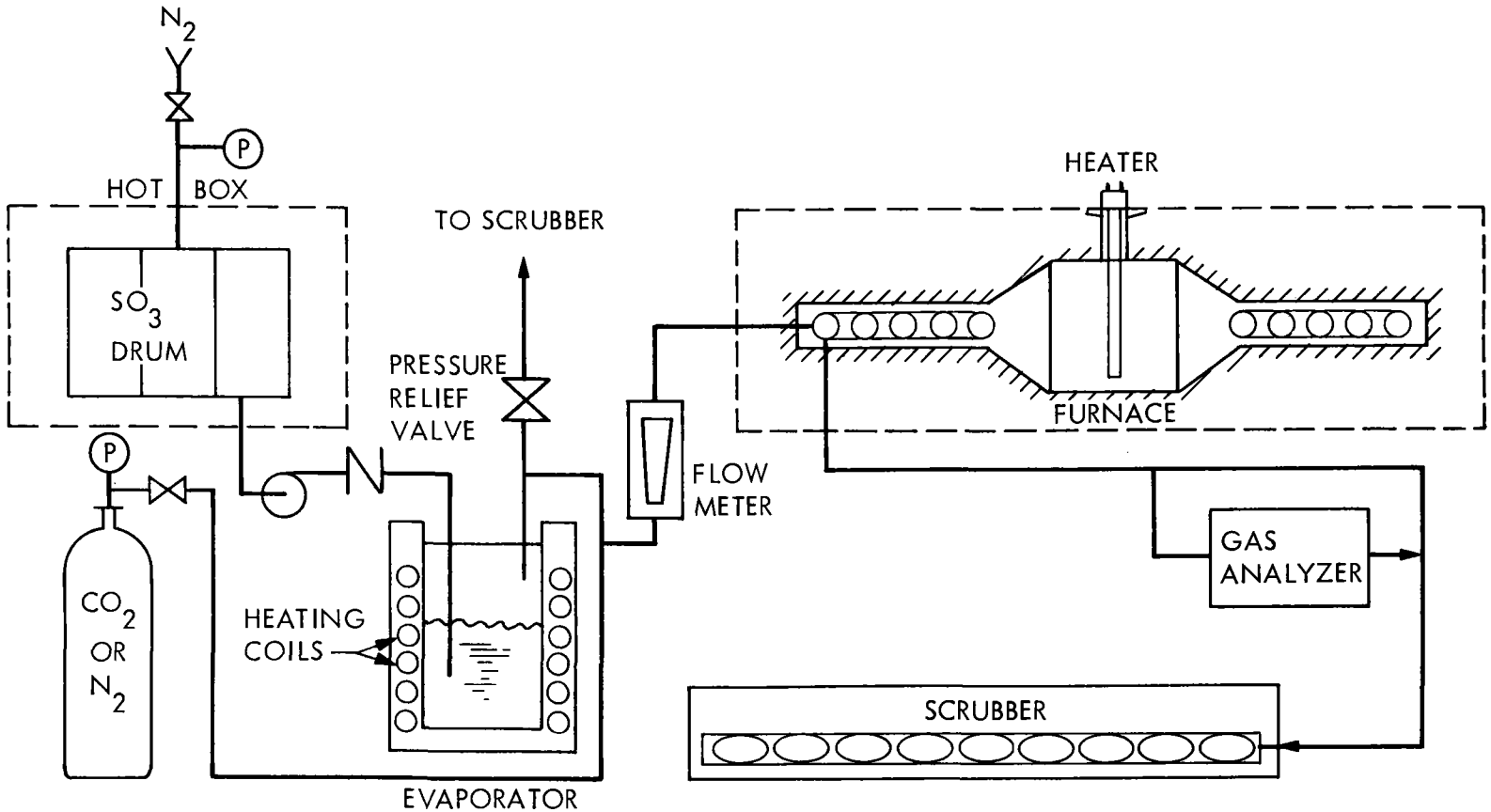

Figure 4-1. Schematic of the Experimental Setup

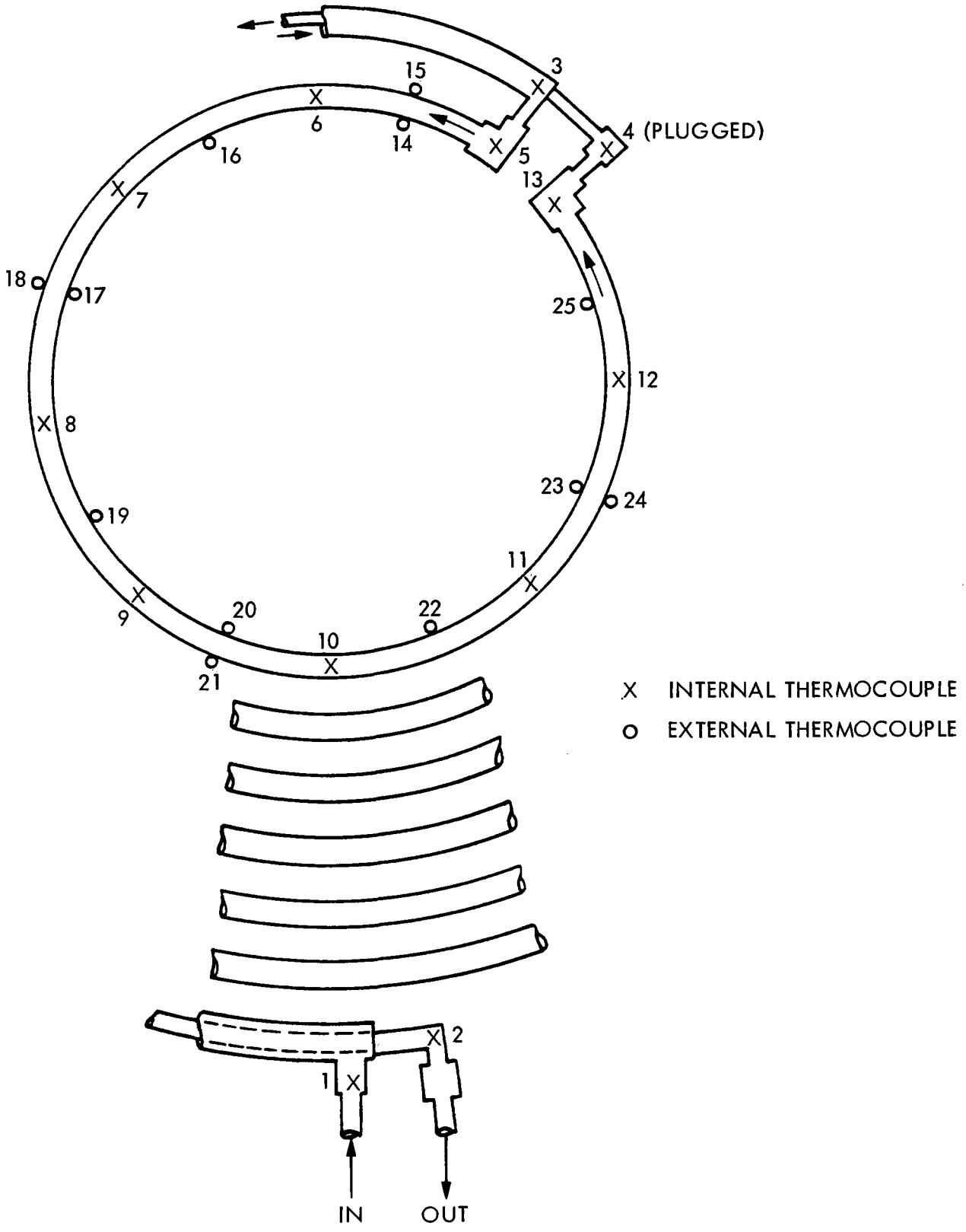

Figure 4-2. Thermocouple Map

Upon completion of the SO_3 conversion tests, the reactor/heat exchanger was disassembled, and the catalyst was removed. Removal of the catalyst was conducted in a controlled manner in order to permit its analysis in reference to its location within the circular reactor. Samples from the inlet and exit sections were analyzed using EDAX (energy dispersive analysis by X-ray). Elemental analyses were conducted at two different energy levels, 20 keV and 40 keV, to examine the relative concentrations of the observed elements at slightly different levels below the surface.

SECTION V

RESULTS AND DISCUSSION

A total of nine test runs, including heat exchanger tests with inert gas, were made at varying flow rates and at maximum temperature. Each run lasted about 90 minutes. At the inception of each of the runs, the system reached steady state in 15 to 20 minutes, but the change of test condition during normal operation was stabilized in a shorter time. Continuous system operation was not possible because of the system fouling problem, which was believed to be caused by the existence of stabilizer in feedstock SO_3. The data measured during each test are the temperature, flow rate, pressure, and SO_2 concentration as a function of time at particular locations of the reactor and/or heat exchanger. A typical example showing the transient system performance is shown in Figures 5-1 through 5-3, where plots of reactant flow rate, three temperatures near the reactor exit end, and the product gas composition are presented. Point-to-point variation in mass flow rate is real and caused by the relatively large gas transit time between the mass flow transducer and the mass flow control valve. It should be noted, however, that when averaged over 10-minute periods, the mass flow is very stable, and these short-term variations do not show up in the temperature and SO_3 concentration data. Reduction of raw data was made by calculating the average quantities during the period of presumed steady state. Figures 5-4 through 5-6 show the fluid stream temperature profile along the reactor length as compared with computed results at three different reactant flow rates and at two or three different heat input levels. At a lower fluid flow rate, the agreement is quite good except at thermocouple position 9 where an exceptionally high temperature was measured. Three possible explanations for this exist: (1) a malfunction of the thermocouple, (2) local overheating due to, perhaps, damaged catalyst, and (3) plugging and redistribution of the gas flow. The discrepancy is more pronounced in cases of higher flow rates as shown in Figures 5-5 and 5-6.

Figure 5-5 is the result of a 2-g/s test at 304 kPa with a reactor maximum temperature of 900°C for one hour. At 30 minutes into the run, thermocouples 12 and 13 rose sharply by over 100°C while thermocouple 9 again measured an abnormally high temperature. This abnormal temperature behavior is attributed to the buildup of deposits of iron or sulfur compounds within the reactor bed causing local heating due to reduced activity. This speculation is further substantiated by the accompanying pressure drop increase observed. Because the power input was controlled by watching the maximum temperature, it is likely that the power input was maintained at an inadvertently low level due to this false T_{max} reading. Indeed, computed results at lower power input agree closely with experimental results.

Figure 5-6 is the result of a 3-g/s test at 304 kPa input pressure and 800°C for 30 minutes followed by 900°C for 30 minutes. Difficulties were encountered during the test; the pressure regulator overheated and the data logger failed to record the outputs from thermocouples 8, 9, 11, and 12. A similar trend of overheating toward the end of reactor bed is observed.

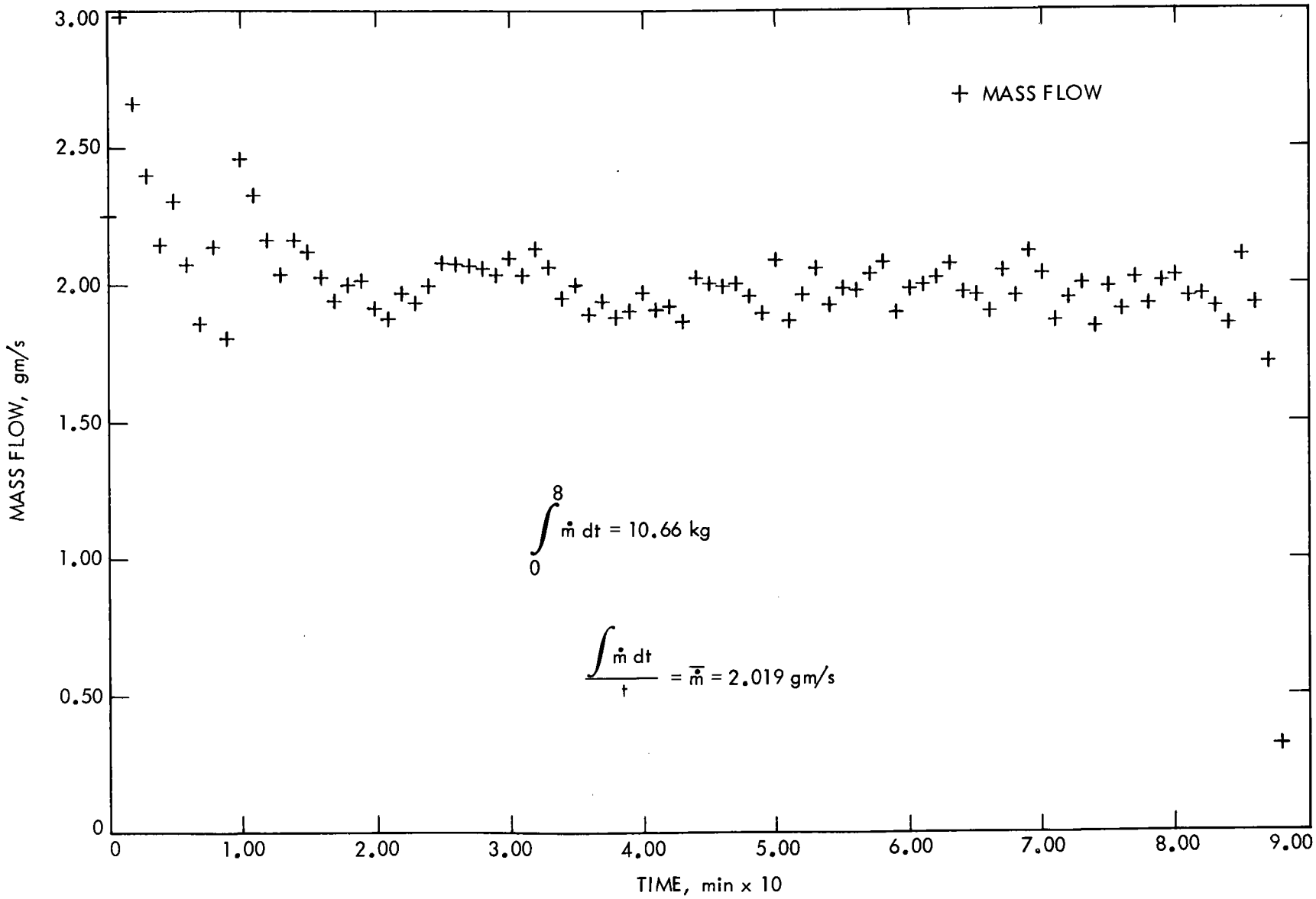

Figure 5-1. Mass Flow Rate As a Function of Time

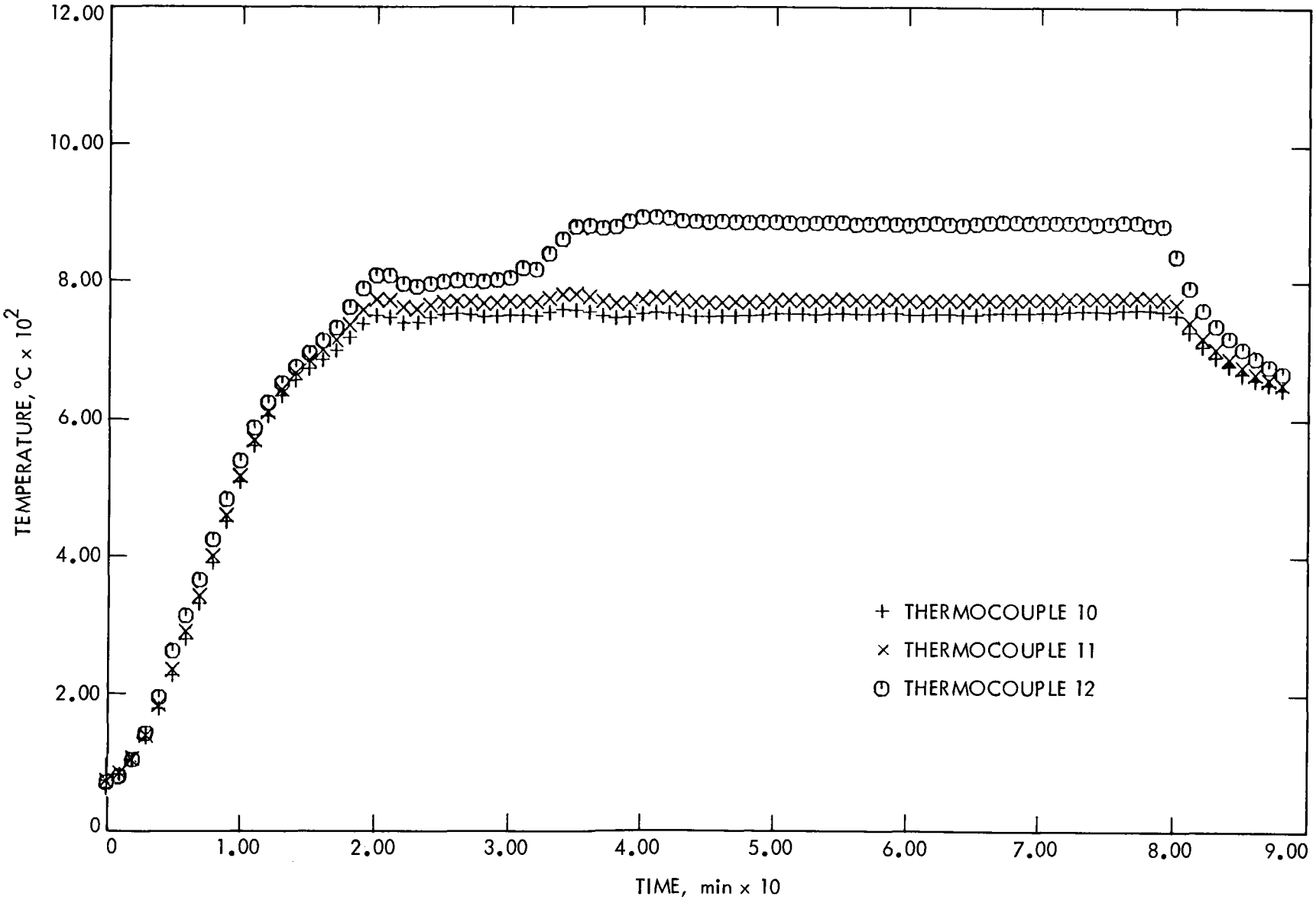

Figure 5-2. Temperature History at Thermocouple Locations 10, 11, and 12

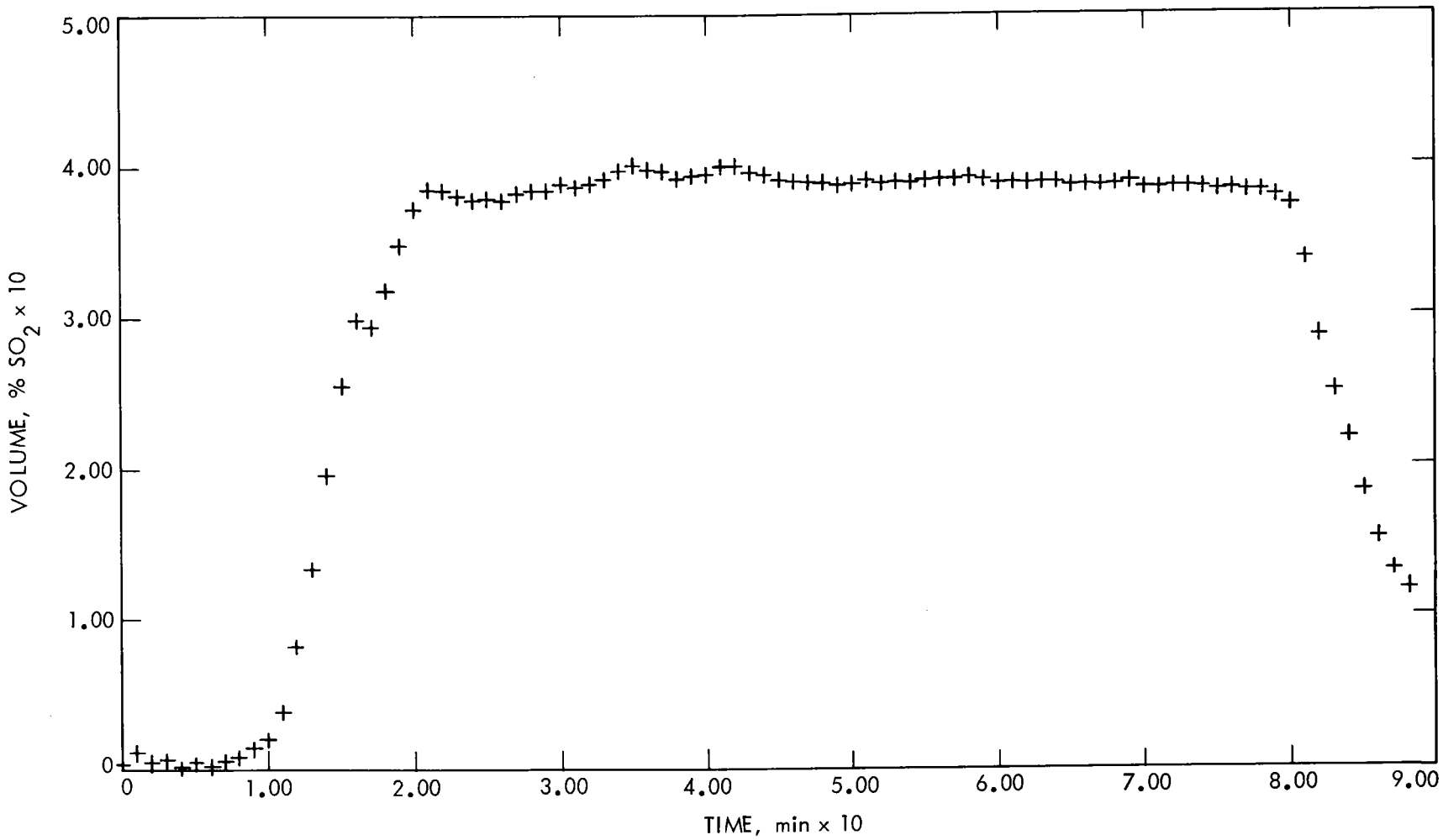

Figure 5-3. SO_2 Concentration in Product Gas As a Function of Time

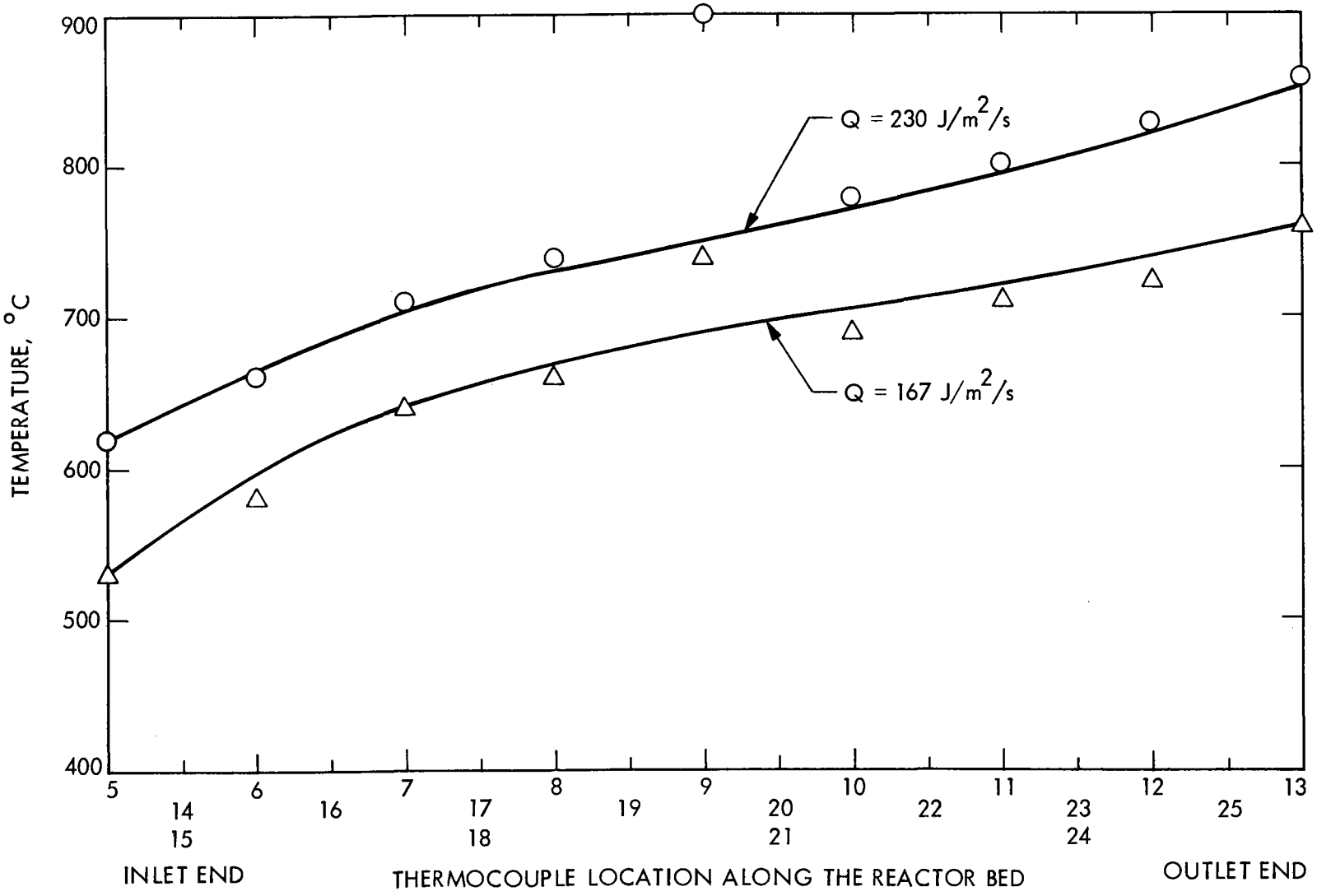

Figure 5-4. Fluid Stream Temperature Profile for $\dot{m}$ = 1 g/s

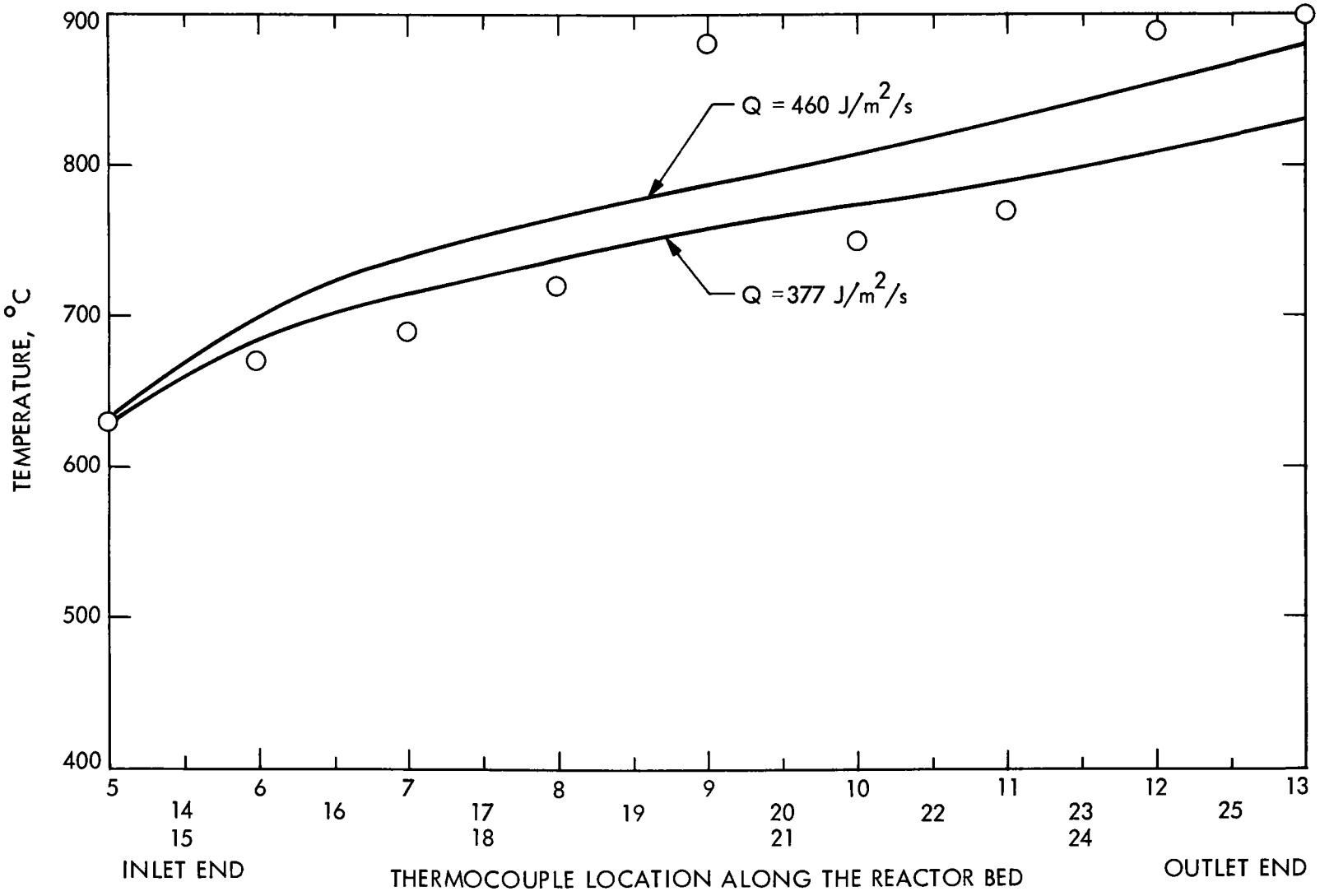

Figure 5-5. Fluid Stream Temperature Profile for $\dot{m}$ = 2 g/s

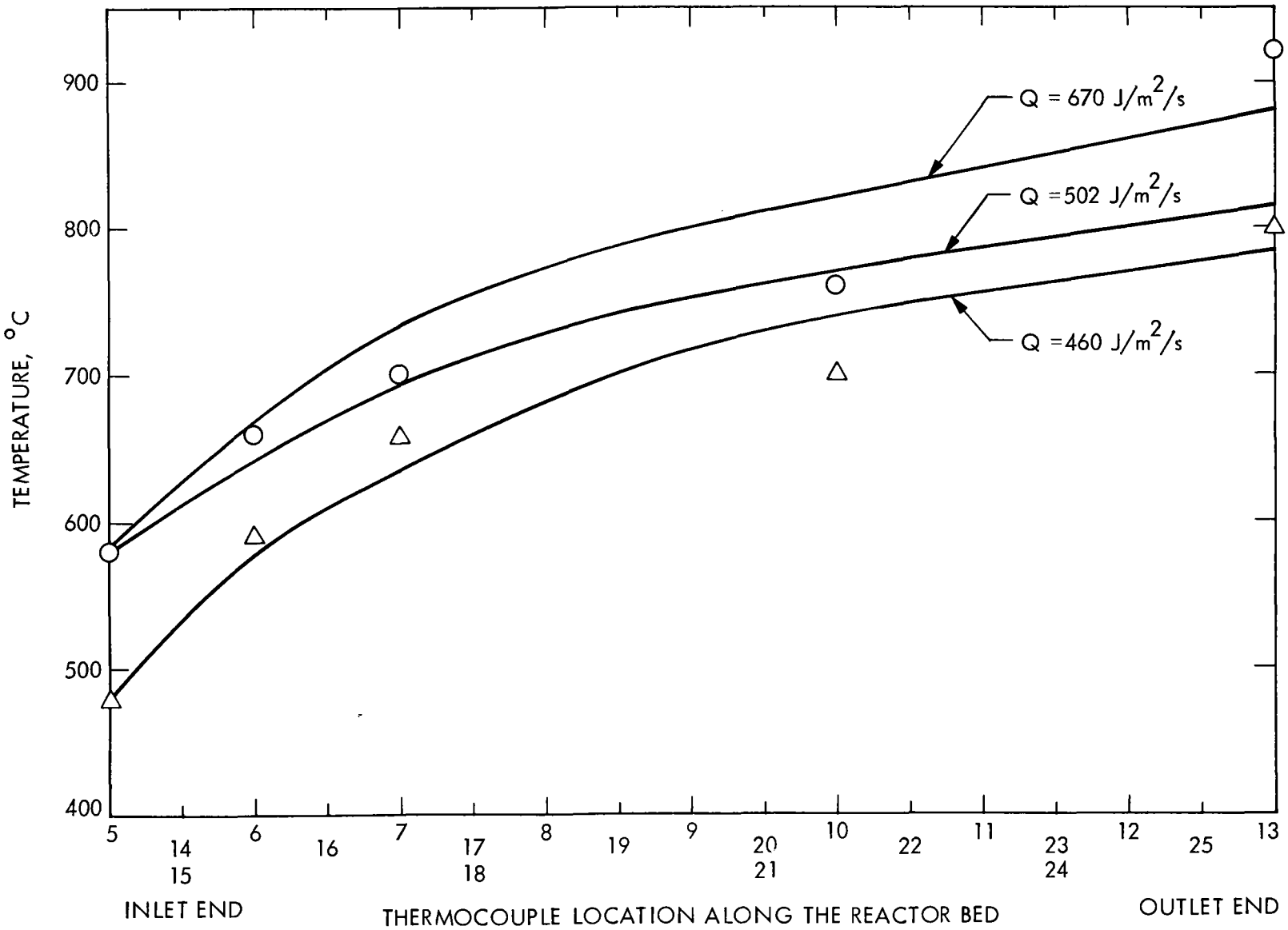

Figure 5-6. Fluid Stream Temperature Profile for $\dot{m}$ = 3 g/s

A summary comparison of pressure drop and extent of reaction is shown in Table 5-1. Conversions range from 23 to 33% of SO_2 mole fraction at a maximum wall temperature of 800°C, and 37 to 40% at a maximum wall temperature of 900°C.

Figure 5-7 is a plot of the experimentally measured extent of reaction compared with calculated results and equilibrium composition at the catalyst surface temperature. The reactant SO_3 enters the converter at a 5-deg angle, and product gases leave at a 355-deg angle. Due to the approximate 90-minute time limit of each run, measurements could be made at only two different angle positions and at the heat exchanger exit. Therefore, extreme care was taken to keep the reaction run conditions constant at an inlet pressure of 304 kPa, a mass flow rate of 2 g/s, and a maximum temperature of 900°C.

One of the key issues in the test program was to determine the potential catalytic effect of bare 316 stainless steel tube on the oxidation of SO_2, the reverse reaction. This test was made by alternately tapping the gas samples from reactor exit and heat exchanger exit and analyzing them. Figure 5-8 shows the result at two different power input levels. As is shown in the figure, no appreciable difference in concentration across a 30-ft-long 316 stainless steel tube is observed in the higher temperature range. Throughout the test, the pressure drop kept increasing as the reaction runs were repeated, but a partial restoration of the flow passage could be made by simply shaking the reactor.

Table 5-1. Comparison of Pressure Drop and Conversion

Run No.	$\dot{m}$, g/s	$T_{w,max}$, °C	ΔP, psi	Conversion, SO_2 Vol % Experimental	Computed
1	1.0	800	2.0 ± 1.0	33.0	29.5
		900	2.1 ± 0.5	40.5	42.5
2	2.0	800	-	-	-
		900	3.5 ± 0.5	39.0	41.5
3	3.0	800	5.5 ± 0.5	24.0	22.5
		900	6.5 ± 1.0	37.0	37.5
4	2.0	800	7.5 ± 1.0	23.0	-
		900	8.5 ± 0.5	37.5	-

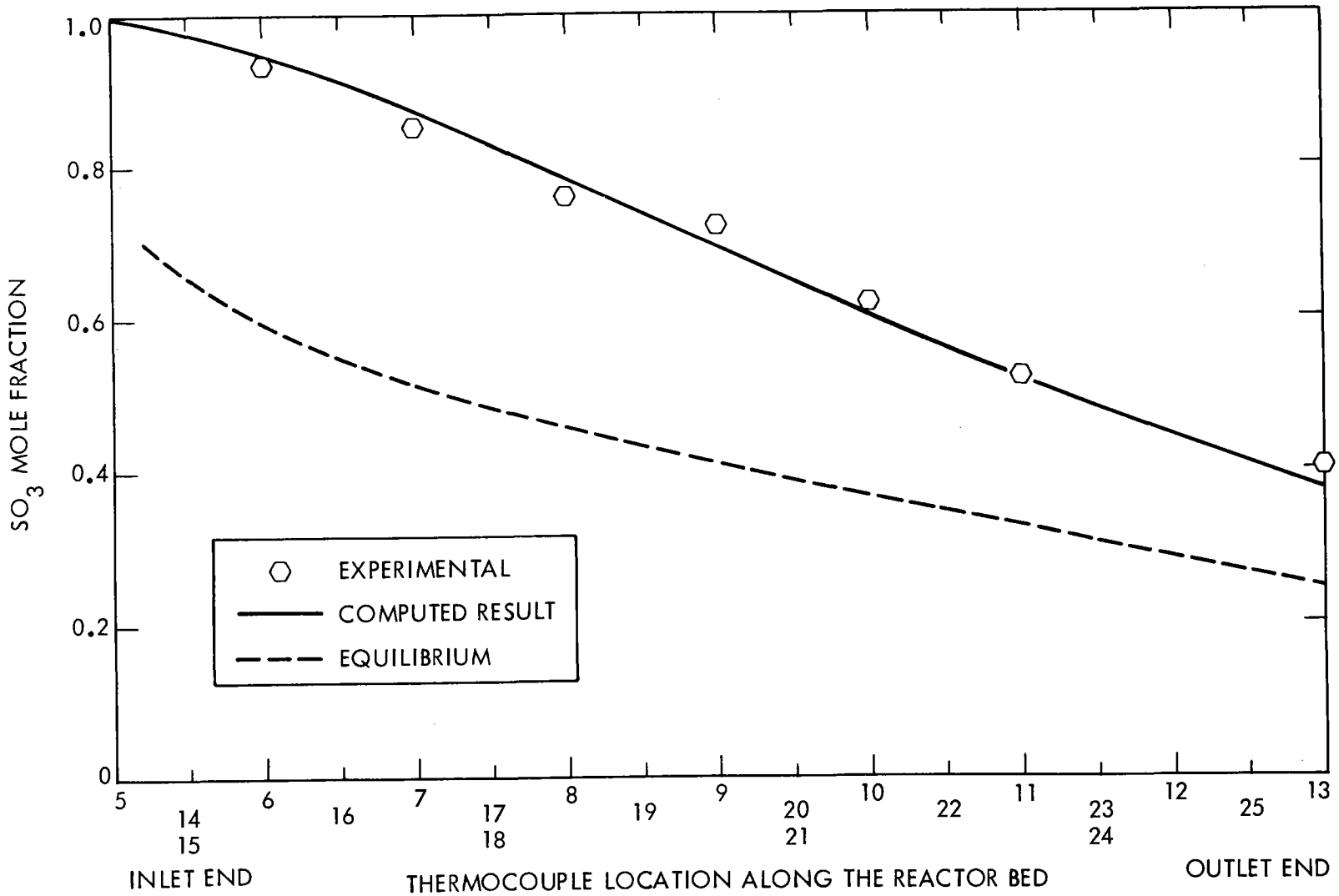

Figure 5-7. Extent of Reaction As a Function of Axial Distance from the Reactor Inlet for $\dot{m}$ = 2 g/s and T_{max} = 900°C

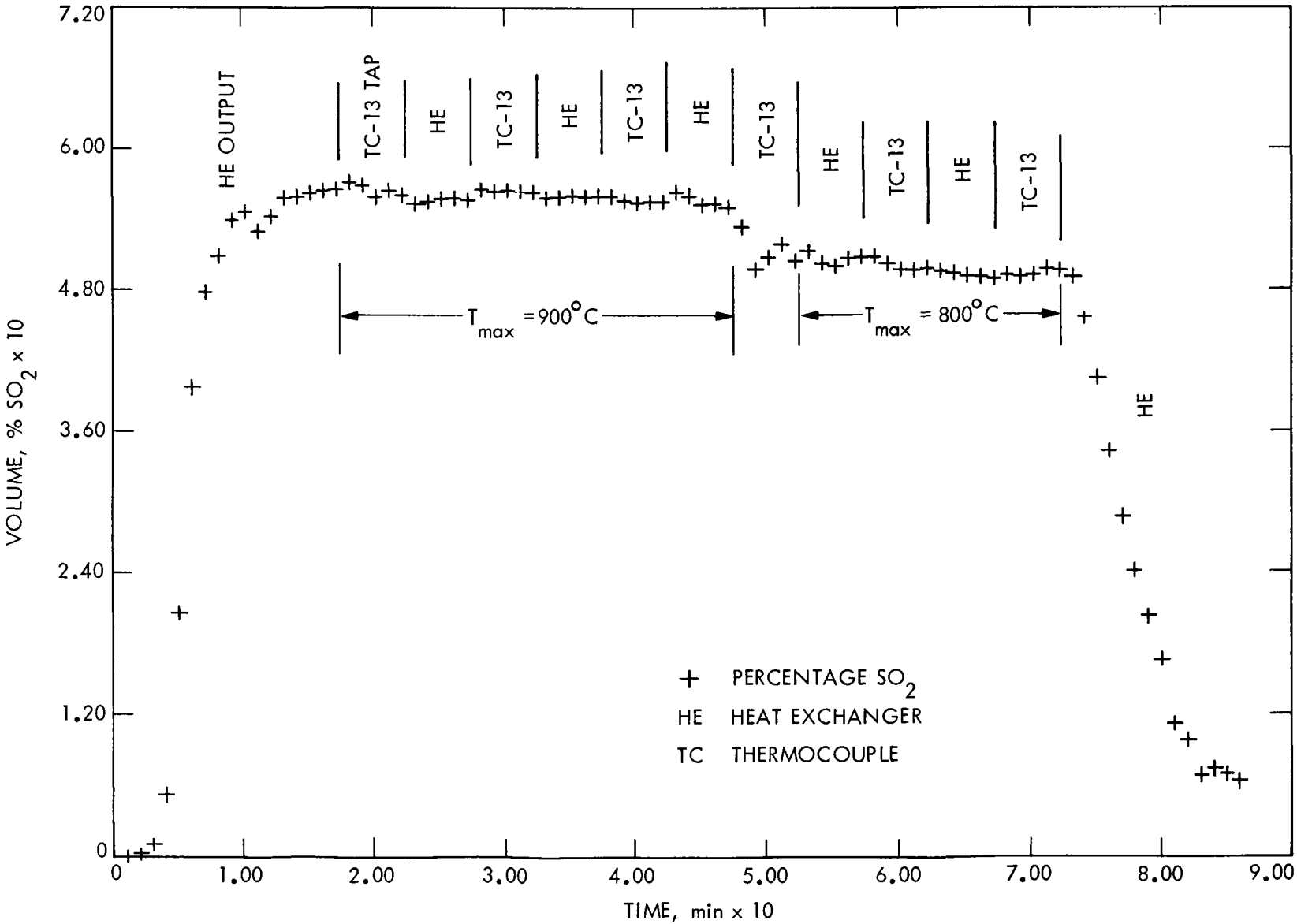

Figure 5-8. Comparison of SO_2 Concentrations at Reactor Exit and Heat Exchanger Exit

The EDAX analysis results with a 20-keV source are shown in Figures 5-9 and 5-10 for the inlet and exit catalyst samples, respectively. Because all the catalyst was prepared uniformly with a 1 wt. % platinum loading on the surface, platinum was used as a comparative standard. The platinum/sulfur peak height ratio is nearly 1/2 in the inlet catalyst sample, while the same ratio is approximately 1/3 in the exit catalyst sample. This indicates that the sulfur content on the surface increases from the inlet to the exit. At the higher beam energy (40 keV) the corresponding ratio found for the inlet sample is 2/3 (Figure 5-11), while for the exit sample the ratio is 1/1 (Figure 5-12). In relative terms, the sulfur has migrated into the catalyst to a lesser extent at the exit section of the bed than at the inlet. However, the penetration of the iron, which originated at the reactor wall, is greater in the exit than in the inlet samples as portrayed by the platinum/iron ratios of 1/1 (at 20 keV) and 2.5/1 (at 40 keV) in the exit sample and of 3/1 and 4/1 in the inlet sample. Detection of chromium in these samples also illustrates the collection of wall material on the catalyst surface.

Large flakes of oxidized stainless steel from the walls of the reactor were found in the catalyst bed, most notably in the center one-third section. In the exit one-third of the reactor, fine material was observed packed in the catalyst spheres along with the wall scale. This material was believed to have contributed to the speculated gas flow restrictions and channelings.

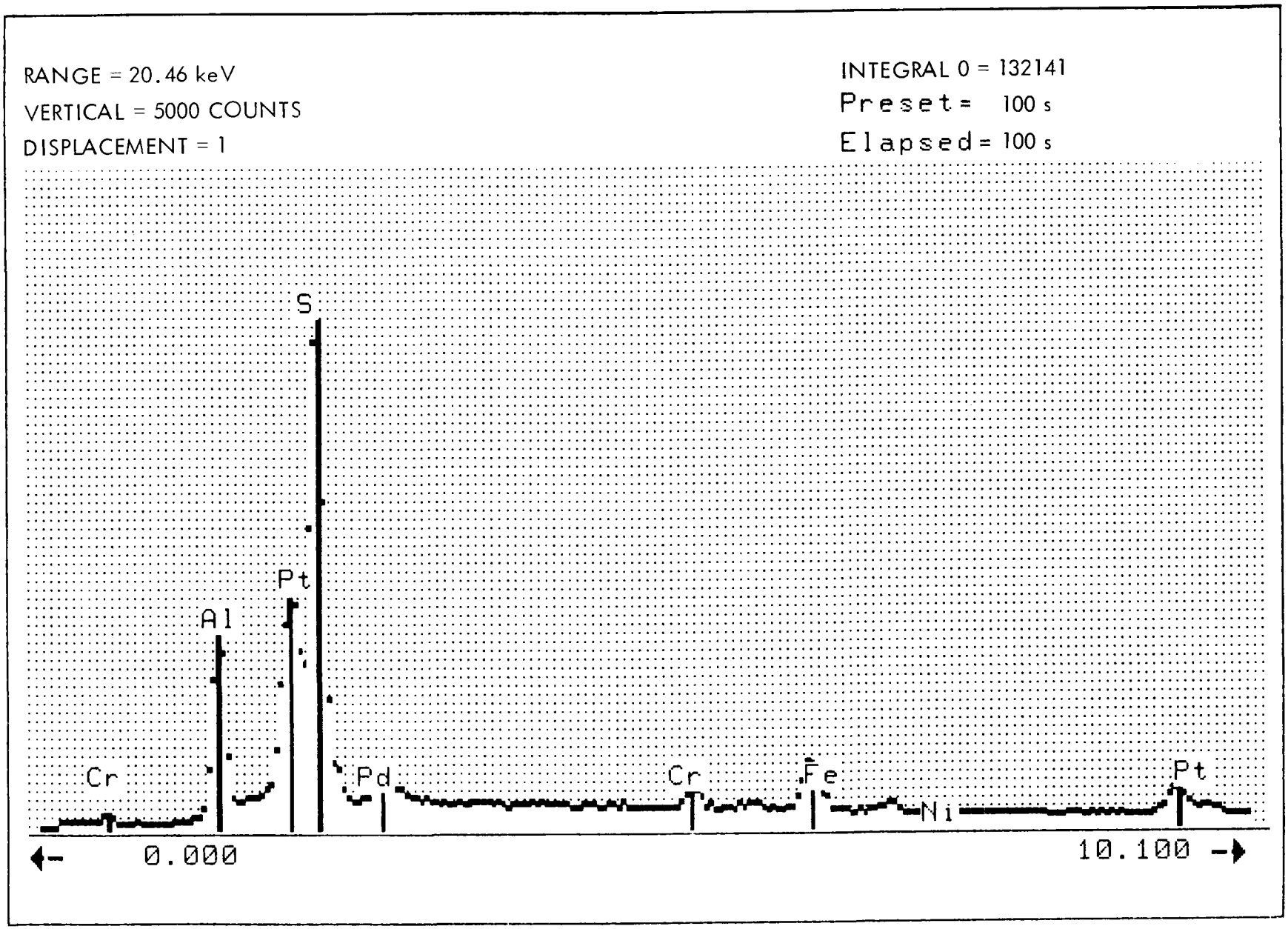

Figure 5-9. Surface Analysis for Inlet Catalyst Samples at a 20-keV Energy Source

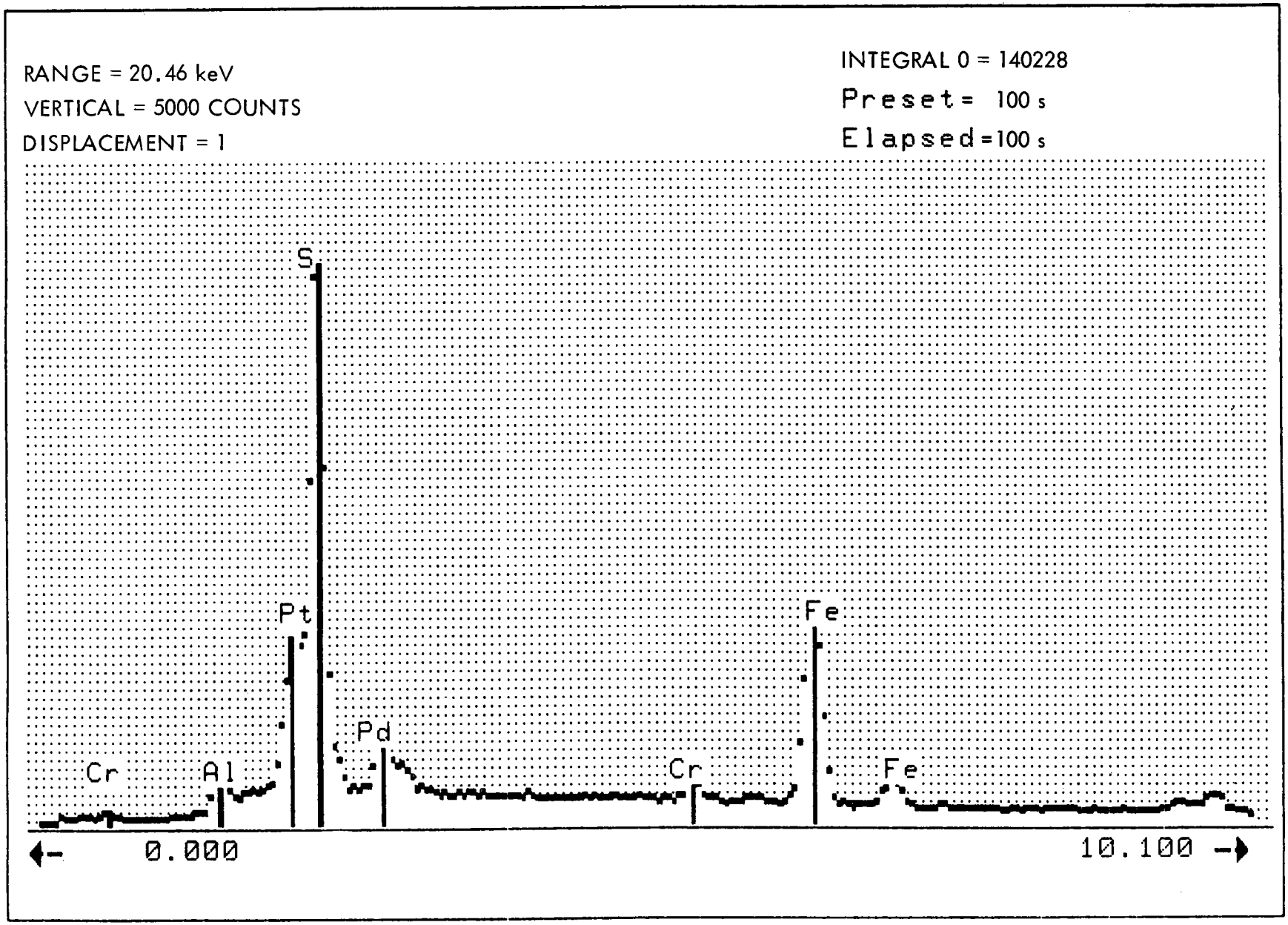

Figure 5-10. Surface Analysis for Exit Catalyst Samples at a 20-keV Energy Source

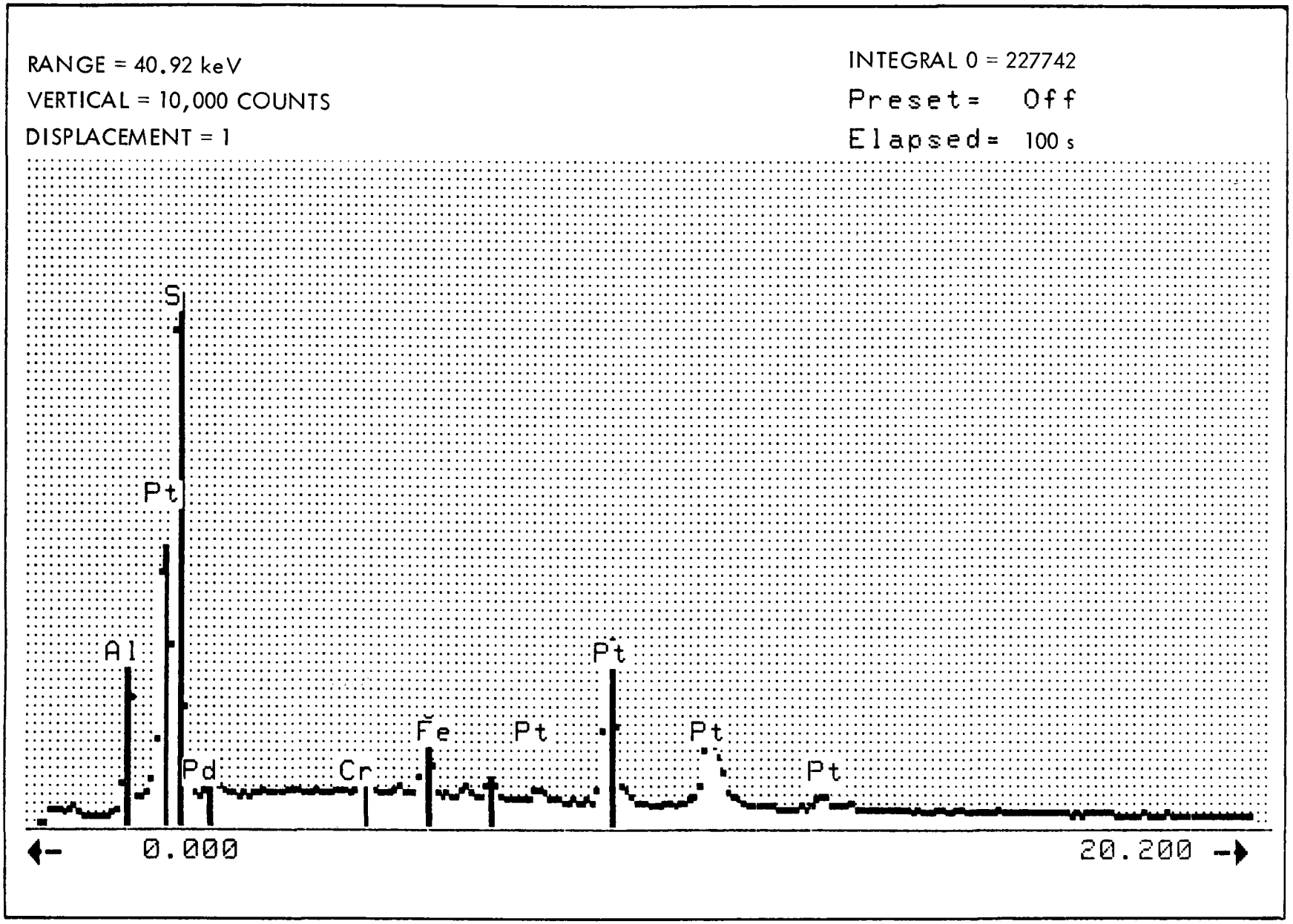

Figure 5-11. Surface Analysis for Inlet Catalyst Samples at a 40-keV Energy Source

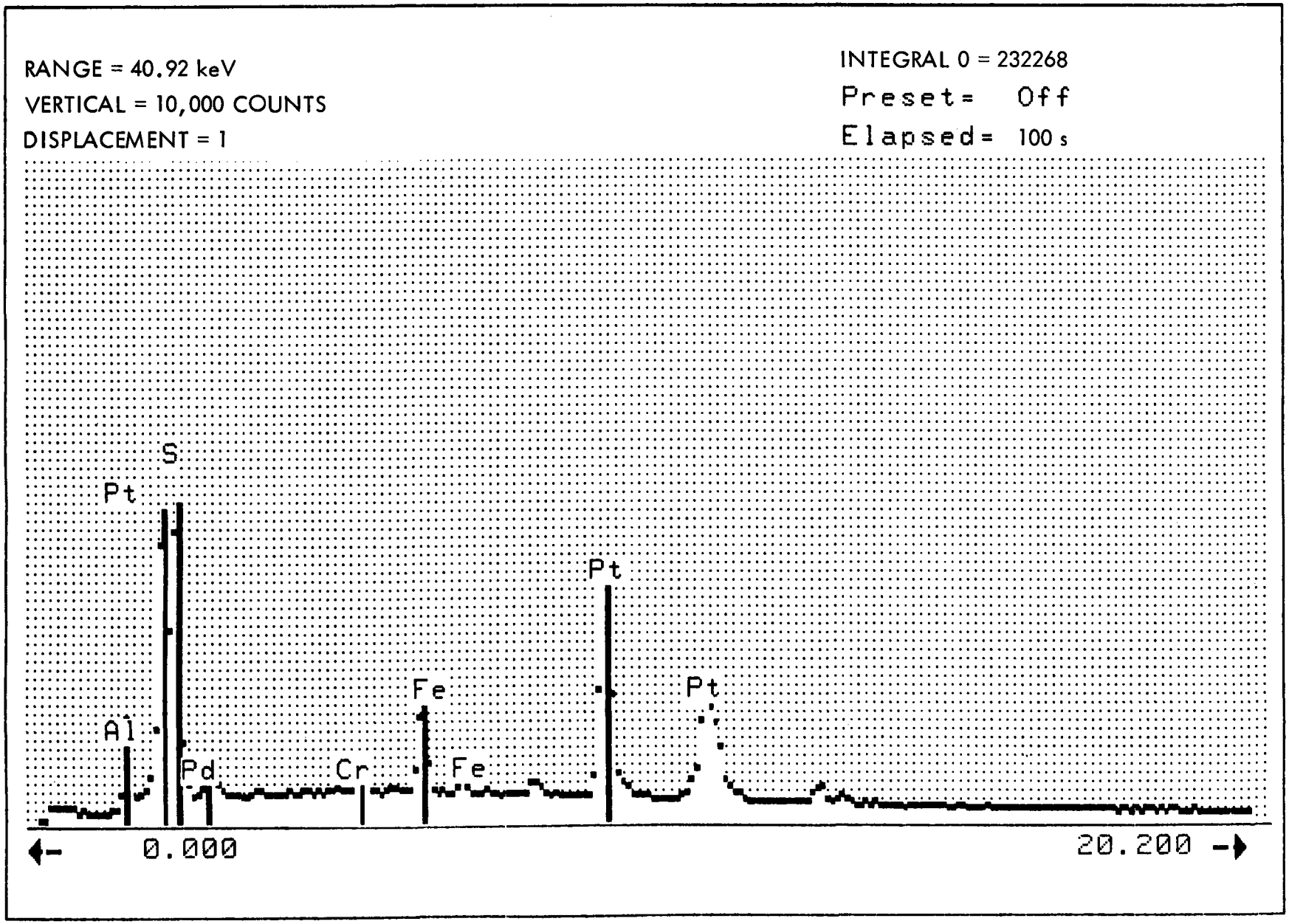

Figure 5-12. Surface Analysis for Exit Catalyst Samples at a 40-keV Energy Source

SECTION VI

CONCLUSION

The receiver design presented herein assures a nominal 10-kW_t conversion capacity and demonstrates the off-design operation flexibility to successfully accommodate the incident radiant energy density profile that the inner wall of the cavity is to be subjected when operating as part of a dish collector system. The developed computer simulation program predicts reasonably well the actual performance and can be used for future design optimization and for techno-economic studies. The catalytic effect of stainless steel tube for the SO_2/O_2 recombination reaction appears to be negligible. At a maximum temperature of about 900°C, the extended use of reactors made of stainless steel (316) appears limited. For long-term reliable operation, units constructed using ceramic material should eventually be developed.

SECTION VII

REFERENCES

1. Chubb, T.A., "Analysis of Gas Dissociation Solar Thermal Power System," Solar Energy, Vol. 17, p. 129, 1975.

2. Chubb, T.A., Nemecek, J.J., and Simmons, D.E., "Application of Chemical Engineering to Large Scale Solar Energy," Solar Energy, Vol. 20, p. 219, 1978.

3. Leva, M., "Packed-Tube Heat Transfer," I & EC, Vol. 42, p. 2498, 1950.

4. Reynolds, W.C., "Heat Transfer to Fully Developed Laminar Flow in a Circular Tube with Arbitrary Circumferential Heat Flux," J. Heat Transf., Vol. 110, May 1960.

5. Farbman, G.H., and Koump, V., Hydrogen Generation Process, Final Report, Advanced Energy Systems Division, Westinghouse Electric Corp., June 1977.

6. Li, C.H., and Schmidt, E.W., "Heat and Mass Transfer Analysis of a Chemical Converter/Heat Exchanger for the SO_2/SO_3 Distributed Solar Energy Collection System," Presented at 1979 International Congress of ISES, Atlanta, Georgia, May 28 to June 1, 1979.

7. McCrary, J.H., Evaluation of Metallic Converters, Test Plan, March 1980.

8. Miyamoto, S., Warrick, A.W., and Bohn, H.L., "Land Disposal of Waste Gas," J. Environmental Quality, Vol. 3, p. 49, 1974.